AJNR

Glioma Grading: Sensitivity, Specificity, and Predictive Values of Perfusion MR Imaging and Proton MR Spectroscopic Imaging Compared with Conventional MR Imaging

Meng Law, Stanley Yang, Hao Wang, James S. Babb, Glyn Johnson, Soonmee Cha, Edmond A. Knopp and David Zagzag

AJNR Am J Neuroradiol 2003, 24 (10) 1989-1998
http://www.ajnr.org/content/24/10/1989

AJNR Am J Neuroradiol 24:1989–1998, November/December 2003

Glioma Grading: Sensitivity, Specificity, and Predictive Values of Perfusion MR Imaging and Proton MR Spectroscopic Imaging Compared with Conventional MR Imaging

Meng Law, Stanley Yang, Hao Wang, James S. Babb, Glyn Johnson, Soonmee Cha, Edmond A. Knopp, and David Zagzag

BACKGROUND AND PURPOSE: **Sensitivity, positive predictive value (PPV), and negative predictive value (NPV) of conventional MR imaging in predicting glioma grade are not high. Relative cerebral blood volume (rCBV) measurements derived from perfusion MR imaging and metabolite ratios from proton MR spectroscopy are useful in predicting glioma grade. We evaluated the sensitivity, specificity, PPV, and NPV of perfusion MR imaging and MR spectroscopy compared with conventional MR imaging in grading primary gliomas.**

METHODS: **One hundred sixty patients with a primary cerebral glioma underwent conventional MR imaging, dynamic contrast-enhanced T2*-weighted perfusion MR imaging, and proton MR spectroscopy. Gliomas were graded as low or high based on conventional MR imaging findings. The rCBV measurements were obtained from regions of maximum perfusion. Metabolite ratios (choline [Cho]/creatine [Cr], Cho/*N*-acetylaspartate [NAA], and NAA/Cr) were measured at a TE of 144 ms. Tumor grade determined with the three methods was then compared with that from histopathologic grading. Logistic regression and receiver operating characteristic analyses were performed to determine optimum thresholds for tumor grading. Sensitivity, specificity, PPV, and NPV for identifying high-grade gliomas were also calculated.**

RESULTS: **Sensitivity, specificity, PPV, and NPV for determining a high-grade glioma with conventional MR imaging were 72.5%, 65.0%, 86.1%, and 44.1%, respectively. Statistical analysis demonstrated a threshold value of 1.75 for rCBV to provide sensitivity, specificity, PPV, and NPV of 95.0%, 57.5%, 87.0%, and 79.3%, respectively. Threshold values of 1.08 and 1.56 for Cho/Cr and 0.75 and 1.60 for Cho/NAA provided the minimum C2 and C1 errors, respectively, for determining a high-grade glioma. The combination of rCBV, Cho/Cr, and Cho/NAA resulted in sensitivity, specificity, PPV, and NPV of 93.3%, 60.0%, 87.5%, and 75.0%, respectively. Significant differences were noted in the rCBV and Cho/Cr, Cho/NAA, and NAA/Cr ratios between low- and high-grade gliomas ($P < .0001$, .0121, .001, and .0038, respectively).**

CONCLUSION: **The rCBV measurements and metabolite ratios both individually and in combination can increase the sensitivity and PPV when compared with conventional MR imaging alone in determining glioma grade. The rCBV measurements had the most superior diagnostic performance (either with or without metabolite ratios) in predicting glioma grade. Threshold values can be used in a clinical setting to evaluate tumors preoperatively for histologic grade and provide a means for guiding treatment and predicting postoperative patient outcome.**

Prospective grading of primary cerebral gliomas is an endeavor with many difficulties but with significant clinical benefit. Despite recent advances in technology, chemotherapeutic agents, radiation therapy options, and surgical techniques, few inroads have been made into improving the survival of patients with malignant gliomas. The mean survival rate remains dismal, with fewer than 10% of patients with glioblas-

Received January 22, 2003; accepted after revision June 11.

Supported by a research grant from the Royal Australian and New Zealand College of Radiologists, Grant RO1CA092992 from the NCI/National Institute of Health.

From the Departments of Radiology (M.L., S.Y., J.S.B., G.J., E.A.K.), Neurosurgery (E.A.K.), and Pathology (D.Z.), New York University Medical Center, NY; the Department of Biostatistics, Fox Chase Cancer Center, Philadelphia, PA (H.W., J.S.B.); and the Department of Radiology, University of California at San Francisco Medical Center, San Francisco, CA (S.C.).

Address reprint requests to Meng Law, MD, Department of Radiology, NYU Medical Center, MR Imaging Dept, Schwartz Bldg, Basement HCC, 530 First Ave, New York, NY 10016.

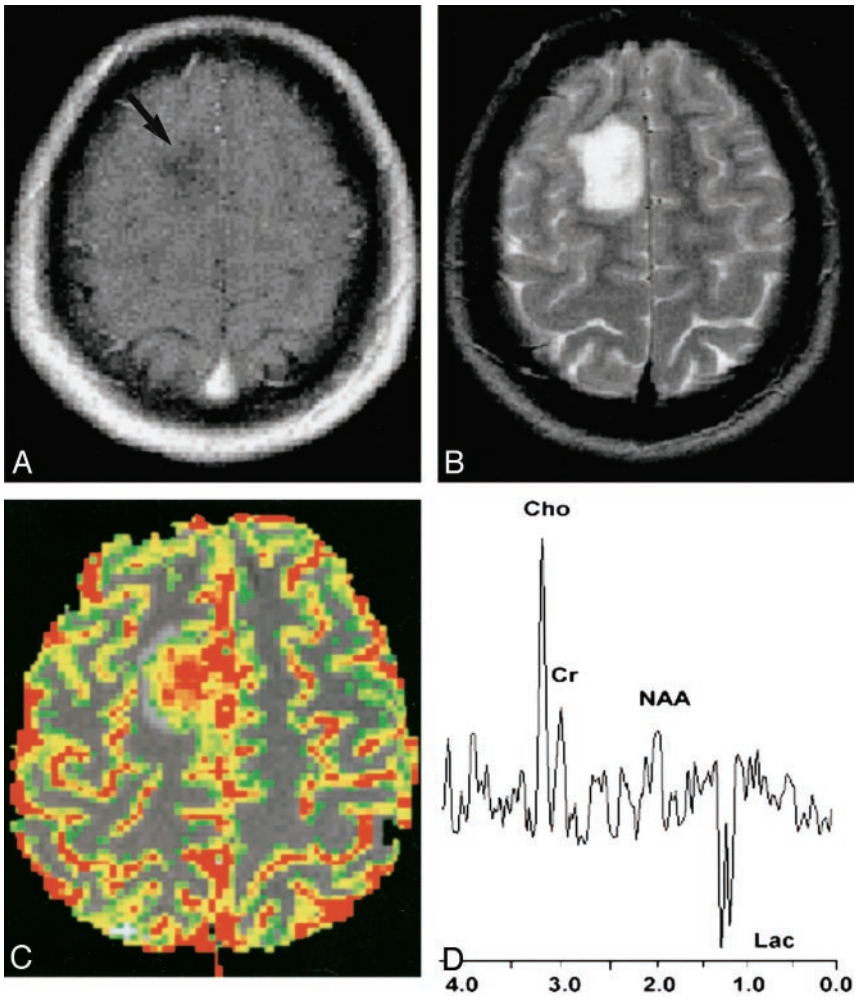

FIG 1. 20-year-old woman with biopsy-proved high-grade glioma.

A, Contrast-enhanced axial T1-weighted image (600/14/1 [TR/TE/NEX]) demonstrates an ill-defined nonenhancing mass (*arrow*) in the right frontal region. The lack of enhancement on the conventional MR image suggests a low-grade glioma.

B, Axial T2-weighted image (3400/119/1) shows increased signal intensity in the mass, with minimal peritumoral edema. This mass was graded as a low-grade glioma with conventional MR imaging because of lack of enhancement, minimal edema, no necrosis, and no mass effect.

C, Gradient-echo (1000/54) axial perfusion MR image with rCBV color overlay map shows increased perfusion with a high rCBV of 7.72, in keeping with a high-grade glioma.

D, Spectrum from proton MR spectroscopy with the PRESS sequence (1500/144) demonstrates markedly elevated Cho and decreased NAA with a Cho/NAA ratio of 2.60, as well as increased lactate (*Lac*), in keeping with a high-grade glioma.

toma multiforme alive after 2 years. Two major limitations are associated with histopathologic grading of gliomas: inherent sampling error associated with stereotactic biopsy and inability to evaluate residual tumor tissue after cytoreductive surgery. Malignant gliomas are known to infiltrate the parenchyma following vascular channels of the white matter tracts (1). This may not be readily appreciated if there is no signal intensity abnormality or enhancement on conventional MR images. Hence, histopathologic grading of gliomas has disadvantages and intrinsic error. The advantage of state-of-the-art MR imaging techniques in evaluating cerebral gliomas is the ability to sample not only the entire lesion, but also the adjacent brain tissue for physiologic and metabolite alterations.

Conventional MR imaging with gadolinium-based contrast agents is an established and useful tool in the characterization of cerebral tumors (2–6). Current 1.5-T clinical MR systems provide excellent anatomic or morphologic imaging of gliomas. However, despite optimization of sequences and protocols, the classification and grading of gliomas with conventional MR imaging is sometimes unreliable, with the sensitivity for glioma grading ranging from 55.1% to 83.3% (7–11). Kondziolka et al (10) demonstrated a 50% false-positive rate in evaluating supratentorial gliomas.

Conventional MR imaging provides important information regarding contrast material enhancement, perienhancement edema, distant tumor foci, hemorrhage, necrosis, mass effect, and so on, which are all helpful in characterizing tumor aggressiveness and hence tumor grade. Dean et al (8) determined that mass effect and necrosis were the two most important predictors of tumor grade. However, often a high-grade glioma may be mistaken for a low-grade glioma when it demonstrates minimal edema, no contrast material enhancement, no necrosis, and no mass effect (Fig 1A and B). Conversely, low-grade gliomas can sometimes demonstrate peritumoral edema, contrast material enhancement, central necrosis, and mass effect and be mistaken for a high-grade glioma (Fig 2A and B). Conventional MR imaging readily provides evidence of contrast material enhancement, signifying blood-brain barrier breakdown, which is often associated with higher tumor grade. However, contrast material enhancement alone is not always accurate in predicting tumor grade. Ginsberg et al (12) demonstrated that lack of enhancement of supratentorial gliomas does not equate with low-grade gliomas. In another study, all low-grade tumors showed contrast material enhancement, but almost one-fifth of glioblastoma multiforme tumors did not (11). The peritumoral hyperintensity on conventional T2-weighted MR images

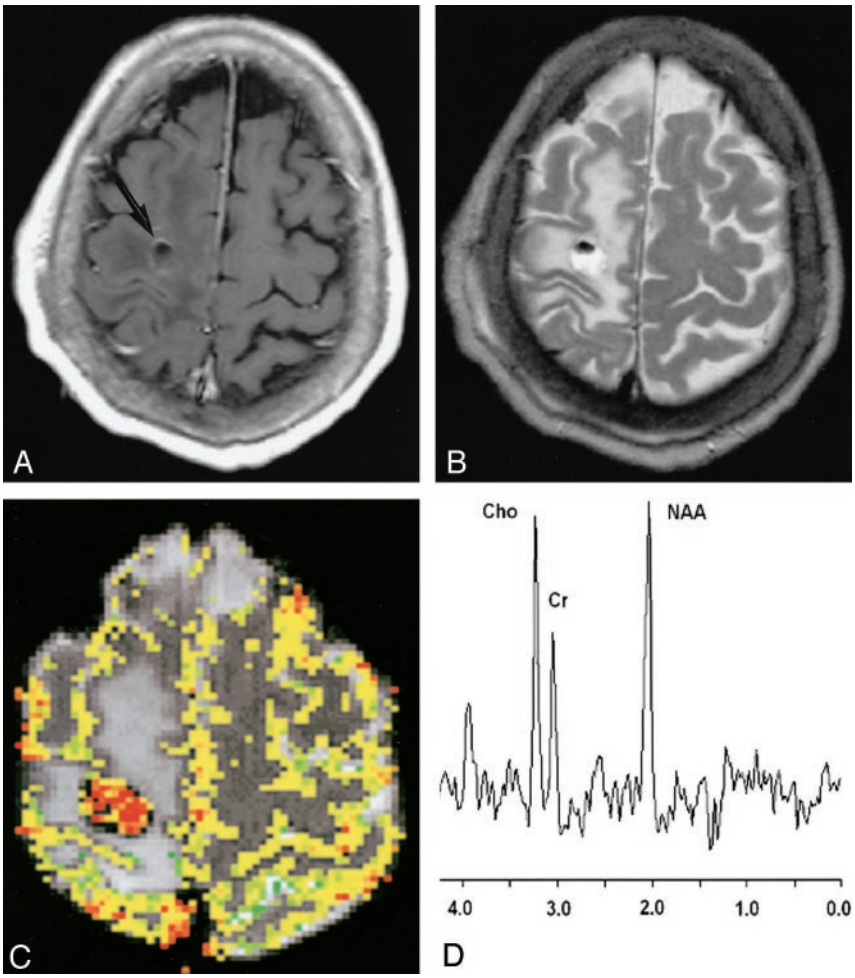

FIG 2. 43-year-old man with biopsy-proved low-grade glioma.

A, Contrast-enhanced axial T1-weighted image (600/14/1) demonstrates a peripherally enhancing mass (*arrow*) in the right frontal region. The presence of contrast material enhancement on the conventional MR image would suggest a high-grade glioma.

B, Axial T2-weighted image (3400/119/1) shows marked peritumoral edema with possible necrosis and blood products. This mass was graded as a high-grade glioma with conventional MR imaging because of the contrast material enhancement, heterogeneity, blood products, possible necrosis, and degree of edema.

C, Gradient-echo (1000/54) axial perfusion MR image with rCBV color overlay map shows a low rCBV of 1.70, in keeping with a low-grade glioma.

D, Spectrum from proton MR spectroscopy with the PRESS sequence (1500/144) demonstrates elevated Cho and slightly decreased NAA with a Cho/NAA ratio of 0.90, which is more in keeping with a low-grade glioma.

is nonspecific, representing tumor infiltration, vasogenic edema, or both. Moreover, conventional MR imaging does not provide reliable information on tumor physiology such as microvascularity, angiogenesis, metabolism, micronecrosis, or cellularity, all of which are also important in determining tumor grade (13–15).

Advanced MR imaging techniques such as perfusion MR imaging and proton MR spectroscopy have found increasing utility in studying brain tumors. Relative cerebral blood volume (rCBV) maps and measurements have been shown to correlate reliably with tumor grade and histologic findings of increased tumor vascularity (11, 16–25). Recent reports regarding MR spectroscopy support its use as a powerful tool in tumor grading as well. Specifically, elevation in choline (Cho) with depression of *N*-acetylaspartate (NAA) is a reliable indicator of tumor. There is extensive literature demonstrating the metabolite ratios of Cho/creatine (Cr), NAA/Cr, and *myo*-inositol/Cr and the presence of lipids and lactate to be useful in grading tumors and predicting tumor malignancy (7, 26–56). There is certainly compelling evidence that MR spectroscopy provides important supplemental information to that of conventional MR imaging. The recent finding of a direct correlation between Cho and Ki-67 levels or cellular proliferative activity provides objective confirmation of the potential of MR spectroscopy in predicting tumor grade (57, 58).

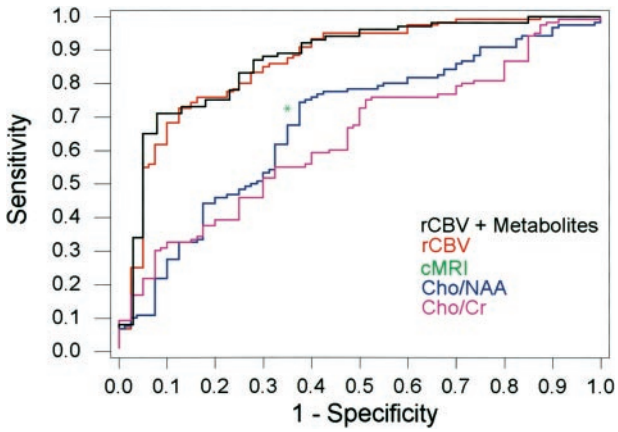

FIG 3. ROC curves for rCBV plus metabolites, rCBV alone, Cho/Cr, and Cho/NAA demonstrate superior sensitivity and specificity of rCBV plus metabolites and rCBV alone compared with conventional MR imaging (*cMRI*, green asterisk) for glioma grading.

To date, there have been some efforts to combine perfusion MR imaging and MR spectroscopic techniques in characterizing gliomas (59, 60). Investigators have also combined these two techniques to evaluate postoperative patients (61) or pediatric patients

with brain tumors (62). Importantly, despite the numerous reports and widespread interest in the characterization of gliomas with these advanced MR imaging techniques, the current clinical role of rCBV and metabolite ratios requires further determination (63). There are surprisingly few reports in the literature describing the false-positive and false-negative rates for glioma grading by using rCBV, metabolite ratios, or both, compared with that for conventional MR imaging. Defining the role of these advanced MR imaging techniques in clinical practice, in terms of the sensitivity, specificity, positive predictive value (PPV), and negative predictive value (NPV), and determining whether perfusion MR imaging, MR spectroscopy, or the combination of the two techniques is more superior need further investigation.

We evaluated our experience in applying both of these advanced techniques in the study of primary cerebral gliomas and compared the sensitivity, specificity, PPV, and NPV of perfusion MR imaging and MR spectroscopy in glioma grading with those of conventional MR imaging. Our purpose was to provide objective data on the clinical utility of perfusion MR imaging and MR spectroscopy in glioma grading and also to proffer some quantitative guidelines for distinguishing low-grade from high-grade gliomas.

Methods

Patients and Histopathologic Analysis

Approval for this study was obtained from the Institutional Board of Research Associates, and informed consent was obtained from all patients. Retrospective analysis of our database of 728 patients who underwent conventional, perfusion, and spectroscopic MR imaging yielded 160 patients who underwent preoperative MR examinations and had histopathologic results for comparison. The conventional MR imaging examinations evaluated were all preoperative. One hundred seventeen patients received their perfusion and spectroscopic imaging before surgery and 43 patients after stereotactic biopsy or partial resection, but the postoperative images demonstrated residual contrast material enhancement. The MR examinations were acquired from November 1999 to July 2002. The patients' ages ranged from 4 to 82 years, with a mean of 43 years. There were 108 male and 52 female patients.

Histopathologic evaluation was performed by an experienced neuropathologist (D.Z.) and was based on a modified Ringertz's three-tier classification of gliomas (64): grade 1, low-grade glioma; grade 2, anaplastic glioma; and grade 3, glioblastoma multiforme. The imaging classification was divided into two tiers. Anaplastic gliomas and glioblastoma multiforme were considered high-grade gliomas, and this group comprised 120 patients. The low-grade gliomas group comprised 40 patients.

Conventional MR Imaging

Imaging was performed with a 1.5-T unit (Vision or Symphony; Siemens AG, Erlangen, Germany). A localizing sagittal T1-weighted image was obtained followed by nonenhanced axial T1-weighted (600/14 [TR/TE]), axial fluid-attenuated inversion-recovery (FLAIR, 9000/110/2500 [TR/TE/TI]), and T2-weighted (3400/119) images. Contrast material–enhanced axial T1-weighted imaging was performed after the acquisition of the perfusion MR imaging data. Two experienced board-certified neuroradiologists (S.Y., E.K.), blinded to the perfusion and MR spectroscopic results, reviewed the conventional MR images and graded each tumor according to the two-tier imaging grading system: low- versus high-grade gliomas. A consensus was reached on the conventional grading of each lesion based on eight criteria: contrast material enhancement, border definition, mass effect, signal intensity heterogeneity, hemorrhage, necrosis, degree of edema, and involvement of the corpus callosum or crossing the midline (8, 9).

Dynamic Contrast-Enhanced Perfusion MR Imaging

Dynamic contrast agent–enhanced T2*-weighted gradient-echo echo-planar images were acquired during the first pass of a standard dose (0.1 mmol/kg) bolus of gadopentetate dimeglumine (Magnevist; Berlex Laboratories, Wayne, NJ). Seven to 10 sections were selected for perfusion MR imaging through the tumor based on T2-weighted and FLAIR images. The methods for acquiring perfusion data from a set of dynamic contrast-enhanced echo-planar images and the precise algorithm for calculating rCBV have been previously described (11). Data processing was performed by using a Unix workstation with analytic programs developed in-house by using C and IDL programming languages. After construction of an rCBV color map to target regions of maximal abnormality, four region-of-interest measurements were obtained, and the maximum rCBV was recorded. This method has been demonstrated to provide the most optimal interobserver and intraobserver reproducibility (65). The standardized region of interest, which measured approximately 2–3 mm^2, was used in most measurements. The rCBV measurements were obtained by a neuroradiologist (G.I.) experienced with perfusion data acquisition at our institution, once again blinded to the conventional and MR spectroscopic findings.

Proton MR Spectroscopic Imaging

Multivoxel 2D proton chemical shift imaging (CSI) or spectroscopic imaging was performed after administration of gadopentetate dimeglumine. This is the standard protocol at our institution, as the literature seems to demonstrate that gadolinium has a negligible effect on metabolite ratios and peak areas (66–68). The volume of interest (VOI) was confirmed by obtaining half-Fourier acquisition single-shot turbo spin-echo images (5/6/500/1 [TR/TE/TI/NEX]). Ten sections with 5-mm section thickness were obtained in 1 minute 15 seconds in the axial, coronal, and sagittal planes for all patients. A volume selective 2D CSI sequence with 1500/144 was used for MR spectroscopic imaging. The hybrid multivoxel CSI technique uses a point-resolved spectroscopy (PRESS) double spin-echo sequence for preselection of a VOI that was usually defined to include the abnormality as well as normal-appearing brain tissue when possible. To prevent strong contribution to the spectra from subcutaneous fat signals, the VOI was completely enclosed within the brain and positioned at the center of the phase-encoded field of view, which was large enough to prevent wraparound artifact. A typical VOI consisted of an 8×8-cm region placed within a 16×16-cm field of view on a 1.5–2-cm transverse section. A 16×16 phase-encoding matrix was used to obtain the 8×8 array of spectra in the VOI, with an in-plane resolution of 1×1 cm and a voxel size of $1 \times 1 \times 1.5$ cm^3 or $1 \times 1 \times 2$ cm^3, depending on the size of the lesion. The metabolite peaks were assigned as follows: Cho, 3.22 ppm; Cr, 3.02 ppm; NAA, 2.02 ppm; mobile lipids, 0.5–1.5 ppm. Lactate was identified at 1.33 ppm by its characteristic doublet that is caused by J modulation and inverted at TE of 144 ms. Metabolite ratios were obtained by a neuroradiologist (M.L.) experienced with spectroscopy and again blinded to the perfusion MR imaging and conventional MR imaging data. Maximal Cho/Cr and Cho/NAA ratios and minimum NAA/Cr ratios were obtained from spectral maps. To ensure quality control and acceptable quality of spectroscopic data, normal values for NAA/Cr and Cho/Cr were obtained in normal-appearing white matter in the contralateral hemisphere.

TABLE 1: Threshold values for rCBV for differentiation between low- and high-grade gliomas

Description	rCBV	Sensitivity	Specificity	PPV	NPV	C2 Error	C1 Error
Minimum C2 Error*	1.75	95.0	57.5	87.0	79.3	14.4	23.8
Minimum C1 Error†	2.97	72.5	87.5	94.6	51.5	23.8	20.0
Same sensitivity as cMRI	2.97	72.5	87.5	94.6	51.5	23.8	20.0
Same specificity as cMRI	2.18	87.5	65.0	88.2	63.4	18.1	23.0

Note.—Conventional MR imaging (cMRI) sensitivity 72.5%, specificity 65.0%, PPV 86.1%, NPV 44.1%, C2 error 29.4%, and C1 error 31.8%.
* C2 = the percentage of observed data points misclassified.
† C1 = 1 − (sensitivity + specificity)/2. This maximizes the average of sensitivity and specificity.

TABLE 2: Threshold values for Cho/Cr ratio for differentiation between low- and high-grade gliomas

Description	Cho/Cr	Sensitivity	Specificity	PPV	NPV	C2 Error	C1 Error
Minimum C2 Error*	1.08	97.5	12.5	77.0	62.5	23.8	45.0
Minimum C1 Error†	1.56	75.8	47.5	81.2	39.6	31.3	38.3
Same sensitivity as cMRI	1.61	72.5	50.0	81.3	37.7	33.1	38.8
Same specificity as cMRI	1.88	55.0	65.0	83.5	33.3	41.9	38.8

Note.—Conventional MR imaging (cMRI) sensitivity 72.5%, specificity 65.0%, PPV 86.1%, NPV 44.1%, C2 error 29.4%, and C1 error 31.8%.
* C2 = the percentage of observed data points misclassified.
† C1 = 1 − (sensitivity + specificity)/2. This maximizes the average of sensitivity and specificity.

Statistical Analysis

Sensitivity, specificity, PPV, and NPV were calculated for correct identification of high-grade gliomas. Hence, tumors classified as high grade and found at histologic examination to be high grade were considered true-positive findings; low-grade gliomas that were histologically confirmed as low grade were considered true-negative findings. For rCBV and metabolite ratios, receiver operating characteristic (ROC) curve analyses were used to evaluate the performance of simple diagnostic tests that declared a glioma to be high grade if and only if the relevant measure (eg, rCBV) for that patient was greater than or equal to some value *K.* This permitted a determination of the sensitivity, specificity, PPV, NPV, and total error associated with each measure as a function of the threshold *K,* used to identify high-grade gliomas. To determine potentially useful threshold values for rCBV, Cho/Cr, and Cho/NAA in differentiating low- from high-grade gliomas, threshold values were found that 1) minimized the observed number of tumor grade misclassifications (C2 error = fraction of misclassified tumors) and 2) maximized the average of the observed sensitivity and specificity (C1 error). Hence, C1 = 1 - (sensitivity + specificity)/2. The Mann-Whitney test was used to compare histologically verified low- and high-grade gliomas in terms of rCBV, Cho/Cr, Cho/NAA, and NAA/Cr. A *P* value less than .05 was considered to indicate a statistically significant difference.

Results

The sensitivity, specificity, PPV, and NPV for determination of a high-grade glioma with conventional MR imaging were 72.5%, 65.0%, 86.1%, and 44.1%, respectively. For a minimum C2 error, a threshold value of 1.75 for rCBV provided sensitivity, specificity, PPV, and NPV of 95.0%, 57.5%, 87.0%, and 79.3%, respectively. For a minimum C1 error, a threshold value of 2.97 for rCBV provided sensitivity, specificity, PPV, and NPV of 72.5%, 87.5%, 94.6%, and 51.5%, respectively (Table 1). A threshold value of 2.97 provided the same sensitivity as that of conventional MR imaging but higher specificity and PPV. A threshold value of 2.18 provided the same specificity as that of conventional MR imaging but higher sensitivity, PPV, and NPV (Table 1).

A threshold value of 1.08 for Cho/Cr provided the minimum C2 error and 97.5%, 12.5%, 77.0%, and 62.5% for the sensitivity, specificity, PPV, and NPV for determination of a high-grade glioma. A threshold value of 1.56 provided the minimum C1 value and 75.8%, 47.5%, 81.2%, and 39.6% for the sensitivity, specificity, PPV, and NPV for determination of a high-grade glioma. Threshold values that provided the same sensitivity and specificity as those of conventional MR imaging were 1.61 and 1.88, respectively (Table 2).

A threshold value of 0.75 for Cho/NAA provided minimum C2 error and 96.7%, 10.0%, 76.3%, and 50.0% for the sensitivity, specificity, PPV, and NPV for determination of a high-grade glioma. A threshold value of 1.6 for Cho/NAA provided minimum C1 error and 74.2%, 62.5%, 85.6%, and 44.6% for the sensitivity, specificity, PPV, and NPV for determination of a high-grade glioma. Threshold values that provided the same sensitivity and specificity as those of conventional MR imaging were 1.66 and 1.78, respectively (Table 3).

The combination of rCBV, Cho/Cr, and Cho/NAA resulted in sensitivity, specificity, PPV, and NPV of 93.3%, 60.0%, 87.5%, and 75%, respectively, for minimum C2 error, and 70.8%, 92.5%, 96.6%, and 51.4%, respectively, for minimum C1 error. For the same sensitivity as that of conventional MR imaging (72.5%), the specificity and PPV were higher, and for the same specificity as that of conventional MR imaging (65.0%), the sensitivity, PPV, and NPV were higher than those of conventional MR imaging alone when using the combination of rCBV, Cho/Cr, and Cho/NAA (Table 4, Fig 3).

The mean, standard deviation, and ranges for rCBV, Cho/Cr, Cho/NAA, and NAA/Cr are shown in Table 5. A statistically significant difference was noted in the rCBV, Cho/Cr, Cho/NAA, and NAA/Cr between low- and high-grade gliomas ($P < .0001$,

TABLE 3: Threshold values for Cho/NAA ratio for differentiation between low- and high-grade gliomas

Description	Cho/NAA	Sensitivity	Specificity	PPV	NPV	C2 Error	C1 Error
Minimum C2 Error*	0.75	96.7	10.0	76.3	50.0	25.0	46.7
Minimum C1 Error†	1.60	74.2	62.5	85.6	44.6	28.8	31.7
Same sensitivity as cMRI	1.66	72.5	62.5	85.3	43.1	30.0	32.5
Same specificity as cMRI	1.78	67.5	65.0	85.3	40.0	33.1	33.8

Note.—Conventional MR imaging (cMRI) sensitivity 72.5%, specificity 65.0%, PPV 86.1%, NPV 44.1%, C2 error 29.4%, and C1 error 31.8%.
* C2 = the percentage of observed data points misclassified.
† C1 = 1 − (sensitivity + specificity)/2. This maximizes the average of sensitivity and specificity.

TABLE 4: rCBV, Cho/Cr ratio, and Cho/NAA ratio together for differentiation between low- and high-grade glioma

Description	Sensitivity	Specificity	PPV	NPV	C2 Error	C1 Error
Minimum C2 Error*	93.3	60.0	87.5	75.0	15.0	23.3
Minimum C1 Error†	70.8	92.5	96.6	51.4	23.7	18.3
Same sensitivity as cMRI	72.5	87.5	94.6	51.5	23.8	20.0
Same specificity as cMRI	89.2	65.0	88.4	66.7	16.9	22.9

Note.—Conventional MR imaging (cMRI) sensitivity 72.5%, specificity 65.0%, PPV 86.1%, NPV 44.1%, C2 error 29.4%, and C1 error 31.8%.
* C2 = the percentage of observed data points misclassified.
† C1 = 1 − (sensitivity + specificity)/2. This maximizes the average of sensitivity and specificity.

TABLE 5: Perfusion MR measure and metabolite ratios for low- and high-grade gliomas and normal values

	Low-Grade Glioma (n = 40)			High-Grade Glioma (n = 120)			
Technique and Measure	Range	Mean	SD	Range	Mean	SD	*P* Value*
Perfusion MR imaging							
rCBV	0.77–9.84	2.14	1.67	0.96–19.80	5.18	3.29	< 0.0001
MR Spectroscopy							
Cho/Cr	0.85–4.00	1.75	0.60	0.83–13.80	2.43	1.92	0.0121
Cho/NAA	0.60–6.80	1.96	1.43	0.53–28.90	3.22	3.65	0.001
NAA/Cr	0.33–3.60	1.20	0.71	0.10–3.93	0.90	0.62	0.0038
Normal values†							
Cho/Cr	0.43–1.37	0.88	0.19	0.44–2.00	0.87	0.24	0.425
NAA/Cr	1.11–2.89	1.72	0.41	0.45–4.74	1.73	0.51	0.958

* Mann-Whitney test.
† Ratios in normal-appearing contralateral brain.

.0121, .001, and .0038, respectively) (Table 5). Within the high-grade glioma group, there were 73 anaplastic gliomas (anaplastic astrocytomas, n = 26; anaplastic oligodendrogliomas, n = 7; anaplastic mixed oligoastrocytomas, n = 40) and 47 glioblastoma multiforme. No statistically significant difference was noted in the rCBV, Cho/Cr, Cho/NAA, and Cho/Cr ratios between the anaplastic gliomas and glioblastoma multiforme groups (P = .549, .302, .363, and .915, respectively).

Discussion

Current methods of grading gliomas have inherent limitations. The current reference standard of histopathologic grading can be inaccurate when biopsy samples are not taken from the most malignant tumor region or when the tumor is not completely resected. This is a particular problem with glioma because of the infiltrative proliferation of the tumor. Although histopathologic grading is often performed on the enhancing portion of the tumor, vascular networks in the peritumoral region serve as a path for tumoral infiltration along perivascular spaces. The region of highest vascularity and malignancy may then be within the so-called peritumoral or perienhancing region (22).

Radiologic grading of tumors with conventional MR imaging is not always accurate, with sensitivity in identifying high-grade gliomas ranging from 55.1% to 83.3% in other studies (7, 8, 11) and 72.5% in this study. Yet, accurate tumor grading has important implications for treatment planning: Patients with an erroneous diagnosis of high-grade glioma will undergo unnecessary adjuvant therapy; patients with an erroneous diagnosis of low-grade glioma will be treated conservatively, with concomitant morbidity and mortality.

Results of several previous studies suggest that rCBV measurements may improve grading. Sugahara et al (18) correlated maximal rCBV values histologically and angiographically in 30 patients, with mean values of 7.32, 5.84, and 1.26 for glioblastomas, anaplastic astrocytomas, and low-grade gliomas, respectively. Aronen et al (16) found mean maximal rCBV values of 3.64 and 1.11 in high- and low-grade glio-

mas, respectively (n = 19). Knopp et al (11) had similar mean maximal rCBV values of 5.07 and 1.44 in high- and low-grade gliomas, respectively (n = 29). These values are comparable to our findings, with mean maximal rCBV values of 5.18 and 2.14 for high- and low-grade gliomas, respectively (Table 5, n = 160). Lev and Rosen (23) used an rCBV threshold value of 1.5 in discriminating among 32 consecutive patients with glioma. Thirteen (100%) of 13 astrocytomas were correctly categorized as high-grade gliomas. Three of these did not enhance after administration of contrast material. Of the nine low-grade astrocytomas, seven were correctly classified. The sensitivity and specificity with use of an rCBV of 1.5 as a threshold value were 100% and 69%, respectively. This compares with the results from this study of 95.0% and 57.5% sensitivity and specificity, respectively, by using 1.75 as the threshold value. More recently, Shin et al (24) demonstrated mean rCBV ratios of 4.91 in high-grade gliomas and 2.00 in low-grade gliomas, in 17 patients; these ratios were similar to the ratios in this study of 5.18 and 2.14 in high- and low-grade gliomas, respectively. The threshold or cutoff value of 2.93 with use of ROC curve analysis is comparable to our value of 2.97 minimizing for C1 error (Table 1).

Besides vascular proliferation, cellularity, mitotic activity, nuclear pleomorphism, and necrosis are important criteria in histopathologic grading of gliomas. Ki-67 labeling is used in histologic examination as a marker for cellular proliferation. A higher rate of Ki-67–positive cells corresponds to greater malignancy in gliomas. Metabolite ratios, in particular Cho levels, have correlated with Ki-67 levels in gliomas (58). MR spectroscopic measurements of Cho/Cr and Cho/NAA ratios should therefore be helpful in the grading of gliomas.

However, to date, there have been few systematic attempts to compare the sensitivity, specificity, PPV, and NPV of perfusion MR imaging and MR spectroscopy with those of conventional MR imaging in glioma grading. To make a comparison, we determined threshold values from logistic regression and ROC analyses. However, it is not always clear what criteria should be used in determining an "optimum" threshold. For example, one could choose to minimize C1 error, which minimizes the average of the false-positive and false-negative error rates. This would be appropriate if the consequence of misclassifying low-grade gliomas is the same as that of misclassifying high-grade gliomas and the two are equally likely to be presented to you for classification. Alternatively, one could choose to minimize the C2 error, the total number of misclassified tumors observed in the data. This adjusts for a difference in the relative frequency of low- and high-grade gliomas in the patient population. In particular, if high-grade gliomas are much more prevalent, then a high misclassification rate of high-grade gliomas would result in a high total number of misclassified gliomas. In the real world, high-grade gliomas are more common than low-grade gliomas. Hence, choosing the threshold to minimize C2 error will tend to yield high sensitivity and relatively low specificity. These are the reasons for presenting two sets of results with threshold values for rCBV and metabolite ratios that minimize both C1 and C2 error values. For application in clinical practice, however, a threshold that minimizes C2 error is most appropriate (Tables 1–3).

The sensitivity of rCBV in glioma grading in our study was 95.0% (minimizing for C2 error), indicating a high true-positive rate and low false-negative rate. Hence, if the rCBV is above 1.75, there is a high probability that the tumor will be a high-grade glioma. Conversely, when rCBV is below 1.75, the tumor is unlikely to be high-grade glioma. However, the relatively low specificity means that false-positive rates are relatively high and true-negative rates are correspondingly low. In other words, some low-grade gliomas will be falsely identified as high-grade gliomas. However, this is the lesser of two evils. First, low-grade gliomas are relatively less common than high-grade gliomas, so fewer errors will be made in absolute terms. Second, a low-grade glioma misidentified as a high-grade glioma will be treated aggressively with some increase in morbidity. However, a high-grade glioma misidentified as a low-grade glioma will be treated conservatively, resulting in potential rapid death.

The high NPV (79.3%) is likewise a significant finding, as gliomas with low rCBV (<1.75) are unlikely to have high-grade components. Hence, it is an excellent tool for excluding the presence of a high-grade glioma (23), an issue that often confronts the neuroradiologist and neuropathologist. The low total error when using rCBV alone suggests that rCBV in itself is an accurate predictor of tumor grade, with a 14.4% chance of error when using 1.75 as the arbitrary threshold value. When one chooses threshold values that demonstrate the same sensitivity as that of conventional MR imaging (72.5%), the specificity, PPV, and NPV are superior to those of conventional MR imaging. Similarly, when one chooses threshold values that demonstrate the same specificity as that of conventional MR imaging (65.0%), the sensitivity, PPV, and NPV are superior to those of conventional MR imaging (Table 1).

The sensitivities (minimized for C2 error) of Cho/Cr and Cho/NAA of 97.5 and 96.7%, respectively, in this study confirm that metabolite ratios can be useful in determining tumor grade. However, the low specificities (12.5% for Cho/Cr and 10.0% for Cho/NAA) are due to the high levels for Cho that we, and others, have observed in some low-grade gliomas. Again, however, high sensitivity in identifying high-grade gliomas is more important than high specificity because of the relatively fewer cases of low-grade glioma and the more serious consequences of false-negative findings.

Despite the low specificities, a significant difference was noted in Cho/Cr, Cho/NAA, and NAA/Cr ratios (P = .012, .001, and .004, respectively) for differentiating between low- and high-grade gliomas (Table 5). A review of the literature, taking into

account differences in MR spectroscopic technique such as the choice of TE and method for determination of metabolite ratios, demonstrates that the mean maximal values obtained for Cho/Cr and Cho/NAA and mean minimum values for NAA/Cr (Table 5) in our study are comparable to previously published data in differentiating between low- and high-grade gliomas (7, 31, 45, 49, 59). Other data in the literature present metabolite levels and direct metabolite concentrations in a slightly different manner than presented in the current study, but they clearly also show differences in Cho levels between low- and high-grade gliomas (35, 54). In the current study, we had a number of reasons for using Cho/Cr and Cho/NAA ratios for assessing tumor grade. First, histopathologically, the linear correlation of Cho with Ki-67 labeling index or cellular proliferative activity suggests that Cho may be a strong predictor of tumor grade (57, 58). Second, although it may be possible to provide better discrimination combining other metabolites such as alanine, lipids, lactate, *myo*-inositol, glutamine, and glutamate, it is often not possible to perform MR spectroscopy at multiple TEs in a clinical setting to provide metabolites such as *myo*-inositol, glutamine, and glutamate detectable best at short TE. Third, to analyze multiple metabolites, linear discriminant analysis (50) or automated spectral analysis software (69) is usually necessary but not commercially available as yet.

One of the challenges in spectroscopy, even with current automated techniques, is obtaining reliable and reproducible intrapatient and interpatient data. To ensure quality control in the data, measurements of normal Cho/Cr and NAA/Cr levels were also obtained in the contralateral unaffected white matter as part of the MR spectroscopy multivoxel, 2D CSI measurement. Despite possible regional variations in metabolite ratios within the brain, it was reassuring to find that normal values for Cho/Cr and Cho/NAA obtained in the low- and high-grade glioma groups were almost identical. Normal Cho/Cr and NAA/Cr levels were 0.88 and 1.72 for low-grade gliomas and 0.87 and 1.73 for high-grade gliomas (Table 5). This not only provides a means for ensuring that the MR spectroscopic data are reliable, but also allows for further comparison between the abnormal data and normative data. In this study, the comparison was made only between low- and high-grade gliomas; however, a comparison between metabolite ratios within the tumor and normal voxels in the same patient is shown in Table 5.

The role of necrosis in glioma grading is important (70). The presence of necrosis is one important distinction between anaplastic astrocytomas and glioblastoma multiforme. In our series, lipid and lactate were found in 5.0% of low-grade gliomas and in 16.6% of high-grade gliomas. There is certainly a difference in finding lipids and lactate between the two groups, and although formal quantification and analyses were not performed in this study, lipids and lactate do correlate with necrosis in high-grade glioma and may also be useful in differentiating glioma grades (27, 45, 71). The frequency of elevated lipid and lactate in the high-grade glioma group was relatively low compared with that of previous studies (45, 71). This may be explained by the population bias in the sample of 73 anaplastic gliomas versus 47 glioblastomas. Furthermore, as this study did not focus on lipids and lactate, formal quantification of these metabolites was not performed, and hence small amounts of lipids and lactate that may be obscured by baseline noise may not be detected.

In a clinical setting, where decisions such as extent of tumoral resection and addition and dose of postoperative chemotherapy, radiation therapy, and interval of follow-up must be made, threshold values can be used as important supplementary information in the noninvasive, neuroradiologic grading of gliomas. A lesion that may have nonspecific conventional MR imaging findings (lack of contrast material enhancement, no mass effect, no necrosis, and no edema), but that demonstrates an rCBV value of 7.72 and Cho/NAA ratio of 2.60, for example, has high sensitivity and specificity for being a high-grade glioma (Fig 1). A comparative lesion (Fig 2) with conventional MR imaging findings suggestive of a high-grade glioma (contrast material enhancement, necrosis, mass effect, and edema) but that demonstrates an rCBV of 1.70 and a Cho/NAA ratio of 0.90 is more in keeping with a low-grade glioma. Hence, using these threshold values in cases that may have nonspecific conventional MR imaging findings increases our confidence in glioma grading.

Of further clinical interest is the differentiation between anaplastic gliomas and glioblastoma multiforme in the high-grade glioma group. As with our findings, previously published data in a group of 26 high-grade gliomas (11) also indicate no significant difference in rCBV between anaplastic astrocytomas and glioblastoma multiforme. Discriminating between these two groups has been demonstrated with in vitro (72) and in vivo (71, 73) MR spectroscopy. A limitation in our study is the perfusion and spectroscopic imaging of a number of patients (n = 43) after surgery. Although it is possible that surgery and postoperative changes may affect tumor vascularity and cellularity, we believe that because these patients only had either partial resection or biopsy, the final statistical analysis would not have been affected greatly by this. We examined the preoperative patients separately, and the results and conclusion did not differ significantly. Another potential limitation of our study is the semiquantification of metabolite ratios by using an internal reference method within the same voxel. The effects of tumor heterogeneity, regional differences in absolute and relative metabolite concentrations, and various pathologies on metabolite T2 relaxation times is difficult to assess. Hence, using Cr as a reference metabolite may increase variability and inaccuracy. Methods to normalize Cho to contralateral normal Cho or contralateral normal Cr as well as methods to provide absolute quantification of metabolites in gliomas have been described (59, 74). Normalizing our results to contralateral normal Cho did

not seem to improve statistical significance substantially; however, it would seem that absolute metabolite quantification methods should improve the sensitivity and possibly the specificity of MR spectroscopy (74). Finally, the lower sensitivity and specificity of Cho compared with rCBV suggests that although Cho levels may correlate directly with tumor cellularity, tumor cellularity may not correlate directly with tumor grade. Tumor grade seems to be more reliably correlated with necrosis, nuclear atypia, mitoses, and vascular hyperplasia (13); hence, rCBV may provide stronger correlation with tumor grade than does Cho.

This study demonstrates that rCBV and metabolite measurements can improve preoperative tumor grading. MR spectroscopy and perfusion MR imaging are useful adjuncts to conventional MR imaging in planning postoperative chemotherapy, antiangiogenic therapy, and radiation therapy (75–77). Since these techniques avoid some of the problems of sampling error associated with histopathologic examination, it is conceivable that such methods may provide a more accurate overall assessment of tumors. Demonstrating that rCBV and MR spectroscopy are sensitive techniques in this study is an important step in this regard. However, the question of whether one can improve the long-term outcome for patients with gliomas remains. Long-term outcome studies are required to determine whether rCBV, Cho levels, or pathology is the best predictor of patient outcome.

Conclusion

Preoperative grading of gliomas based on conventional MR imaging is often unreliable. Independently and in combination, rCBV measurements and Cho/Cr and Cho/NAA ratios can significantly improve the sensitivity and predictive values of preoperative glioma grading. The rCBV measurements are the best parameter for glioma grading. This is extremely important for determining the most optimal therapy regimen and the regularity and aggressiveness of postoperative follow-up and treatment. At our institution, perfusion MR imaging and MR spectroscopy not only have become a routine part of glioma imaging, but also have become an important adjunctive tool in providing information in gliomas and regions of the brain that may have eluded histopathologic assessment. Perfusion MR imaging and MR spectroscopy can potentially overcome the limitation of sampling error with histopathologic grading of tumor by the ability to sample the entire lesion noninvasively in vivo. Ongoing data collection from longitudinal studies is crucial to determine if rCBV and metabolite ratios can, in the long run, be comparable to histopathologic examination in predicting tumor behavior and patient prognosis.

References

1. Kelly PJ, Daumas-Duport C, Scheithauer BW, et al. **Stereotactic histologic correlations of computed tomography- and magnetic resonance imaging-defined abnormalities in patients with glial neoplasms.** *Mayo Clin Proc* 1987;62:450–459
2. Brant-Zawadzki M, Berry I, Osaki L, et al. **Gd-DTPA in clinical MR of the brain: I. Intraaxial lesions.** *AJR Am J Roentgenol* 1986; 147:1223–1230
3. Brant-Zawadzki M, Badami JP, Mills CM, et al. **Primary intracranial tumor imaging: a comparison of magnetic resonance and CT.** *Radiology* 1984;150:435–440
4. Bydder GM, Steiner RE, Young IR, et al. **Clinical NMR imaging of the brain: 140 cases.** *AJR Am J Roentgenol* 1982;139:215–236
5. Just M, Thelen M. **Tissue characterization with T1, T2, and proton density values: results in 160 patients with brain tumors.** *Radiology* 1988;169:779–785
6. Felix R, Schorner W, Laniado M, et al. **Brain tumors: MR imaging with gadolinium-DTPA.** *Radiology* 1985;156:681–688
7. Moller-Hartmann W, Herminghaus S, Krings T, et al. **Clinical application of proton magnetic resonance spectroscopy in the diagnosis of intracranial mass lesions.** *Neuroradiology* 2002;44:371–381
8. Dean BL, Drayer BP, Bird CR, et al. **Gliomas: classification with MR imaging.** *Radiology* 1990;174:411–415
9. Watanabe M, Tanaka R, Takeda N. **Magnetic resonance imaging and histopathology of cerebral gliomas.** *Neuroradiology* 1992;34: 463–469
10. Kondziolka D, Lunsford LD, Martinez AJ. **Unreliability of contemporary neurodiagnostic imaging in evaluating suspected adult supratentorial (low-grade) astrocytoma.** *J Neurosurg* 1993;79:533–536
11. Knopp EA, Cha S, Johnson G, et al. **Glial neoplasms: dynamic contrast-enhanced T2*-weighted MR imaging.** *Radiology* 1999;211: 791–798
12. Ginsberg LE, Fuller GN, Hashmi M, et al. **The significance of lack of MR contrast enhancement of supratentorial brain tumors in adults: histopathological evaluation of a series.** *Surg Neurol* 1998; 49:436–440
13. Daumas-Duport C, Scheithauer B, O'Fallon J, et al. **Grading of astrocytomas: a simple and reproducible method.** *Cancer* 1988;62: 2152–2165
14. Burger PC, Vogel FS, Green SB, et al. **Glioblastoma multiforme and anaplastic astrocytoma: pathologic criteria and prognostic implications.** *Cancer* 1985;56:1106–1111
15. Burger P. **Malignant astrocytic neoplasms: classification, pathology, anatomy, and response to therapy.** *Semin Oncol* 1986;13:16–20
16. Aronen HJ, Gazit IE, Louis DN, et al. **Cerebral blood volume maps of gliomas: comparison with tumor grade and histologic findings.** *Radiology* 1994;191:41–51
17. Bruening R, Kwong KK, Vevea MJ, et al. **Echo-planar MR determination of relative cerebral blood volume in human brain tumors: T1 versus T2 weighting.** *AJNR Am J Neuroradiol* 1996;17:831–840
18. Sugahara T, Korogi Y, Kochi M, et al. **Correlation of MR imaging-determined cerebral blood volume maps with histologic and angiographic determination of vascularity of gliomas.** *AJR Am J Roentgenol* 1998;171:1479–1486
19. Sugahara T, Korogi Y, Shigematsu Y, et al. **Value of dynamic susceptibility contrast magnetic resonance imaging in the evaluation of intracranial tumors.** *Top Magn Reson Imaging* 1999;10:114–124
20. Wong ET, Jackson EF, Hess KR, et al. **Correlation between dynamic MRI and outcome in patients with malignant gliomas.** *Neurology* 1998;50:777–781
21. Wong JC, Provenzale JM, Petrella JR. **Perfusion MR imaging of brain neoplasms.** *Am J Roentgenol* 2000;174:1147–1157
22. Cha S, Knopp EA, Johnson G, et al. **Intracranial mass lesions: dynamic contrast-enhanced susceptibility-weighted echo-planar perfusion MR imaging.** *Radiology* 2002;223:11–29
23. Lev MH, Rosen BR. **Clinical applications of intracranial perfusion MR imaging.** *Neuroimaging Clin N Am* 1999;9:309–331
24. Shin JH, Lee HK, Kwun BD, et al. **Using relative cerebral blood flow and volume to evaluate the histopathologic grade of cerebral gliomas: preliminary results.** *Am J Roentgenol* 2002;179:783–789
25. Petrella JR, Provenzale JM. **MR perfusion imaging of the brain: techniques and applications.** *Am J Roentgenol* 2000;175:207–219
26. Adamson AJ, Rand SD, Prost RW, et al. **Focal brain lesions: effect of single-voxel proton MR spectroscopic findings on treatment decisions.** *Radiology* 1998;209:73–78
27. Alger JR, Frank JA, Bizzi A, et al. **Metabolism of human gliomas: assessment with H-1 MR spectroscopy and F- 18 fluorodeoxyglucose PET.** *Radiology* 1990;177:633–641
28. Arnold DL, Shoubridge EA, Villemure JG, et al. **Proton and phosphorus magnetic resonance spectroscopy of human astrocytomas in vivo: preliminary observations on tumor grading.** *NMR Biomed* 1990;3:184–189

29. Bruhn H, Frahm J, Gyngell ML, et al. **Noninvasive differentiation of tumors with use of localized H-1 MR spectroscopy in vivo: initial experience in patients with cerebral tumors.** *Radiology* 1989;172: 541–548
30. Castillo M, Kwock L. **Clinical applications of proton magnetic resonance spectroscopy in the evaluation of common intracranial tumors.** *Top Magn Reson Imaging* 1999;10:104–113
31. Castillo M, Smith JK, Kwock L. **Correlation of *myo*-inositol levels and grading of cerebral astrocytomas.** *AJNR Am J Neuroradiol* 2000;21:1645–1649
32. Chang L, McBride D, Miller BL, et al. **Localized in vivo 1H magnetic resonance spectroscopy and in vitro analyses of heterogeneous brain tumors.** *J Neuroimaging* 1995;5:157–163
33. Cheng LL, Chang IW, Louis DN, et al. **Correlation of high-resolution magic angle spinning proton magnetic resonance spectroscopy with histopathology of intact human brain tumor specimens.** *Cancer Res* 1998;58:1825–1832
34. Danielson ER, Ross BD. **Magnetic Resonance Spectroscopy of Neurological Diseases.** New York, NY: Marcel Dekker Inc., 1998
35. Dowling C, Bollen AW, Noworolski SM, et al. **Preoperative proton MR spectroscopic imaging of brain tumors: correlation with histopathologic analysis of resection specimens.** *AJNR Am J Neuroradiol* 2001;22:604–612
36. Falini A, Calabrese G, Origgi D, et al. **Proton magnetic resonance spectroscopy and intracranial tumours: clinical perspectives.** *J Neurol* 1996;243:706–714
37. Fountas KN, Kapsalaki EZ, Gotsis SD, et al. **In vivo proton magnetic resonance spectroscopy of brain tumors.** *Stereotact Funct Neurosurg* 2000;74:83–94
38. Fulham MJ, Bizzi A, Dietz MJ, et al. **Mapping of brain tumor metabolites with proton MR spectroscopic imaging: clinical relevance.** *Radiology* 1992;185:675–686
39. Kaminogo M, Ishimaru H, Morikawa M, et al. **Diagnostic potential of short echo time MR spectroscopy of gliomas with single-voxel and point-resolved spatially localised proton spectroscopy of brain.** *Neuroradiology* 2001;43:353–363
40. Kugel H, Heindel W, Ernestus RI, et al. **Human brain tumors: spectral patterns detected with localized H-1 MR spectroscopy.** *Radiology* 1992;183:701–709
41. Butzen J, Prost R, Chetty V, et al. **Discrimination between neoplastic and nonneoplastic brain lesions by use of proton MR spectroscopy: the limits of accuracy with a logistic regression model.** *AJNR Am J Neuroradiol* 2000;21:1213–1219
42. Luyten PR, Marien AJ, Heindel W, et al. **Metabolic imaging of patients with intracranial tumors: H-1 MR spectroscopic imaging and PET.** *Radiology* 1990;176:791–799
43. McBride DQ, Miller BL, Nikas DL, et al. **Analysis of brain tumors using 1H magnetic resonance spectroscopy.** *Surg Neurol* 1995;44: 137–144
44. McKnight TR, Noworolski SM, Vigneron DB, et al. **An automated technique for the quantitative assessment of 3D-MRSI data from patients with glioma.** *J Magn Reson Imaging* 2001;13:167–177
45. Meyerand ME, Pipas JM, Mamourian A, et al. **Classification of biopsy-confirmed brain tumors using single-voxel MR spectroscopy.** *AJNR Am J Neuroradiol* 1999;20:117–123
46. Negendank WG, Sauter R, Brown TR, et al. **Proton magnetic resonance spectroscopy in patients with glial tumors: a multicenter study.** *J Neurosurg* 1996;84:449–458
47. Nelson SJ. **Analysis of volume MRI and MR spectroscopic imaging data for the evaluation of patients with brain tumors.** *Magn Reson Med* 2001;46:228–239
48. Ott D, Hennig J, Ernst T. **Human brain tumors: assessment with in vivo proton MR spectroscopy.** *Radiology* 1993;186:745–752
49. Poptani H, Gupta RK, Roy R, et al. **Characterization of intracranial mass lesions with in vivo proton MR spectroscopy.** *AJNR Am J Neuroradiol* 1995;16:1593–1603
50. Preul MC, Caramanos Z, Collins DL, et al. **Accurate, noninvasive diagnosis of human brain tumors by using proton magnetic resonance spectroscopy.** *Nat Med* 1996;2:323–325
51. Rand SD, Prost R, Haughton V, et al. **Accuracy of single-voxel proton MR spectroscopy in distinguishing neoplastic from nonneoplastic brain lesions.** *AJNR Am J Neuroradiol* 1997;18:1695–1704
52. Ross B, Michaelis T. **Clinical applications of magnetic resonance spectroscopy.** *Magn Reson Q* 1994;10:191–247
53. Rutter A, Hugenholtz H, Saunders JK, et al. **Classification of brain tumors by ex vivo 1H NMR spectroscopy.** *J Neurochem* 1995;64: 1655–1661
54. Shimizu H, Kumabe T, Tominaga T, et al. **Noninvasive evaluation of malignancy of brain tumors with proton MR spectroscopy.** *AJNR Am J Neuroradiol* 1996;17:737–747
55. Tedeschi G, Lundbom N, Raman R, et al. **Increased choline signal coinciding with malignant degeneration of cerebral gliomas: a serial proton magnetic resonance spectroscopy imaging study.** *J Neurosurg* 1997;87:516–524
56. Wilken B, Dechent P, Herms J, et al. **Quantitative proton magnetic resonance spectroscopy of focal brain lesions.** *Pediatr Neurol* 2000; 23:22–31
57. Tamiya T, Kinoshita K, Ono Y, et al. **Proton magnetic resonance spectroscopy reflects cellular proliferative activity in astrocytomas.** *Neuroradiology* 2000;42:333–338
58. Shimizu H, Kumabe T, Shirane R, et al. **Correlation between choline level measured by proton MR spectroscopy and Ki-67 labeling index in gliomas.** *AJNR Am J Neuroradiol* 2000;21:659–665
59. Yang D, Korogi Y, Sugahara T, et al. **Cerebral gliomas: prospective comparison of multivoxel 2D chemical- shift imaging proton MR spectroscopy, echoplanar perfusion and diffusion-weighted MRI.** *Neuroradiology* 2002;44:656–666
60. Law M, Cha S, Knopp EA, et al. **High-grade gliomas and solitary metastases: differentiation by using perfusion and proton spectroscopic MR imaging.** *Radiology* 2002;222:715–721
61. Henry RG, Vigneron DB, Fischbein NJ, et al. **Comparison of relative cerebral blood volume and proton spectroscopy in patients with treated gliomas.** *AJNR Am J Neuroradiol* 2000;21:357–366
62. Tzika AA, Vajapeyam S, Barnes PD. **Multivoxel proton MR spectroscopy and hemodynamic MR imaging of childhood brain tumors: preliminary observations.** *AJNR Am J Neuroradiol* 1997;18: 203–218
63. Lev MH. **Gliomatosis cerebri has normal relative blood volume: really?! Who cares? Should you?** *AJNR Am J Neuroradiol* 2002;23: 345–346
64. Ringertz J. **Grading of gliomas.** *Acta Pathol Microbiol Scand* 1950; 27:51–64
65. Wetzel SG, Cha S, Johnson G, et al. **Relative cerebral blood volume measurements in intracranial mass lesions: interobserver and intraobserver reproducibility study.** *Radiology* 2002;224:797–803
66. Lin AP, Ross BD. **Short-echo time proton MR spectroscopy in the presence of gadolinium.** *J Comput Assist Tomogr* 2001;25:705–712
67. Murphy PS, Dzik-Jurasz AS, Leach MO, et al. **The effect of Gd-DTPA on T1-weighted choline signal in human brain tumours.** *Magn Reson Imaging* 2002;20:127–130
68. Smith JK, Kwock L, Castillo M. **Effects of contrast material on single-volume proton MR spectroscopy.** *AJNR Am J Neuroradiol* 2000;21:1084–1089
69. Tate AR, Majos C, Moreno A, et al. **Automated classification of short echo time in in vivo 1H brain tumor spectra: a multicenter study.** *Magn Reson Med* 2003;49:29–36
70. Nelson JS, Tsukada Y, Schoenfeld D, et al. **Necrosis as a prognostic criterion in malignant supratentorial, astrocytic gliomas.** *Cancer* 1983;52:550–554
71. Li X, Lu Y, Pirzkall A, et al. **Analysis of the spatial characteristics of metabolic abnormalities in newly diagnosed glioma patients.** *J Magn Reson Imaging* 2002;16:229–237
72. Carpinelli G, Carapella CM, Palombi L, et al. **Differentiation of glioblastoma multiforme from astrocytomas by in vitro 1H MRS analysis of human brain tumors.** *Anticancer Res* 1996;16:1559–1563
73. McKnight TR, von dem Bussche MH, Vigneron DB, et al. **Histopathological validation of a three-dimensional magnetic resonance spectroscopy index as a predictor of tumor presence.** *J Neurosurg* 2002;97:794–802
74. Isobe T, Matsumura A, Anno I, et al. **Quantification of cerebral metabolites in glioma patients with proton MR spectroscopy using T2 relaxation time correction.** *Magn Reson Imaging* 2002;20:343–349
75. Cha S, Knopp EA, Johnson G, et al. **Dynamic contrast-enhanced T2-weighted MR imaging of recurrent malignant gliomas treated with thalidomide and carboplatin.** *AJNR Am J Neuroradiol* 2000; 21:881–890
76. Nelson SJ, Huhn S, Vigneron DB, et al. **Volume MRI and MRSI techniques for the quantitation of treatment response in brain tumors: presentation of a detailed case study.** *J Magn Reson Imaging* 1997;7:1146–1152
77. Nelson SJ, Vigneron DB, Dillon WP. **Serial evaluation of patients with brain tumors using volume MRI and 3D 1H MRSI.** *NMR Biomed* 1999;12:123–138